

# Will RANS Survive LES? A View of Perspectives

**K. Hanjalic**

e-mail: hanjalic@ws.tn.tudelft.nl  
Thermal and Fluids Sciences,  
Department of Multi-scale Physics,  
Delft University of Technology,  
Lorentzweg 1, 2628 CJ Delft,  
The Netherlands

*The paper provides a view of some developments and a perspective on the future role of the Reynolds-averaged Navier-Stokes (RANS) approach in the computation of turbulent flows and heat transfer in competition with large-eddy simulations (LES). It is argued that RANS will further play an important role, especially in industrial and environmental computations, and that the further increase in the computing power will be used more to utilize advanced RANS models to shorten the design and marketing cycle rather than to yield the way to LES. We also discuss some current and future developments in RANS aimed at improving their performance and range of applicability, as well as their potential in hybrid approaches in combination with the LES strategy. Limitations in LES at high Reynolds ( $Re$ ) and Rayleigh ( $Ra$ ) number flows and heat transfer are revisited and some hybrid RANS/LES routes are discussed. The potential of very large eddy simulations (VLES) of flows dominated by (pseudo)-deterministic eddy structures, based on transient RANS (T-RANS) and similar approaches, is discussed and illustrated in an example of “ultra-hard” (very high  $Ra$ ) thermal convection. [DOI: 10.1115/1.2037084]*

*Keywords:* Turbulence Modeling, Convective Heat Transfer RANS, T-RANS, LES, Hybrid RANS-LES

## Introduction

Despite their disputable intuitive and empirical rationale, the one-point turbulence closures for Reynolds-averaged Navier-Stokes (RANS) equations have remained for over three decades the mainstay of the industrial computational fluid dynamics (CFD). They are simple to use, computationally affordable, and economical, thus appealing to industry for various applications such as design, optimization, prediction of off-design performances, or for predicting the outcome in situations that are inaccessible to experiment or to other simulation methods. But, as it is well known, the most popular and most widely used linear eddy-viscosity models (EVMs) have serious fundamental deficiencies and cannot be trusted for predicting genuinely new situations of realistic complexity. Various modifications and new modeling concepts have been proposed over the past decades, ranging from ad hoc remedies, complex nonlinear eddy-viscosity approaches to multi-equation and multi-scale second-moment closures (SMCs) (Reynolds stress/flux, algebraic, or differential models). No consensus has ever been reached—and probably it never will—on what should be the optimum model(s) or level of closure. A broad palette of RANS variants are currently used and some models—primarily at the simple EVM level seem to have found niches in different areas of application. However, a general feeling among many CFD users is that the RANS have not met with early expectation. Alternatives have been sought in other approaches, questioning the RANS future and disputing its current role as the only viable tool for industrial and environmental computations of complex turbulent flows and transport phenomena.

The developments in direct and large eddy simulations (DNS, LES) have opened new prospects. While DNS has been viewed as an indispensable research tool, LES has been expected to emerge as the future industrial standard, threatening to eliminate RANS. This excitement did not last for long: while LES proved to be certainly a powerful method, because of formidable demands on grid resolution its application is and will for long be limited to low-to-moderate  $Re$  and  $Ra$  numbers and relatively simple geometries. Handling the wall-bounded flows, with focus on wall phe-

nomena, friction and heat and mass transfer, especially at high  $Re$  and  $Ra$  numbers, poses great challenge. For such situations, combining the advantages of RANS and LES seems at present—at least for some flow types—the best option. Because such hybrid approaches imply numerical resolution in time and space of *only* very large eddies (VLES) while the significant portion of turbulence spectrum needs to be modeled, the modeling of the unresolved (“subscale”) motion requires a more sophisticated approach than used for common LES subgrid-scale models, opening thus a new niche for the RANS modeling. These prospects, as well as the realization that the grid resolution problem of LES will make this technique long inapplicable to large-scale industrial and environmental problems, have recently renewed the interest in further improvement of RANS and RANS-based methods, as well as their combination with the LES strategy.

We begin with a brief discussion of the current status, limitations, and possible developments of the RANS and related approaches in view of the future increase in the computing power. Some genuine niches for LES, inaccessible to RANS methods (and also for experiments), are then discussed. As an example we discuss the problem of the accurate prediction of distribution and time variation of the surface temperature in configurations encountered in electronics cooling, in internal cooling of gas turbine blades, or other similar applications. Here the local hot spots or strong time variation of the surface temperature and the consequent thermal fatigue are regarded as the major cause of equipment malfunctioning. We move then to discuss some developments in RANS modeling for complex flows and convective heat transfer. By noting some promising progress in numerical treatment of advanced RANS models, primarily at the second-moment level, we show some successful applications of these models to complex flows of industrial relevance, as well as some recent novelties in the model developments originating from the author’s group. A new, robust variant of the elliptic relaxation eddy-viscosity model,  $k-\varepsilon-\zeta-f$ , is presented, followed by a new second-moment “elliptic blending” closure. As an example of successful application in the forced convection problem, we consider multiple jets impinging normally on a flat surface, which are used frequently to achieve efficient cooling or heating of solid walls. The attention is then turned to the combination of RANS with LES (hybrid RANS/LES). Several noted controversial issues are

Contributed by the Fluids Engineering Division for publication in the JOURNAL OF FLUIDS ENGINEERING. Manuscript received by the Fluids Engineering Division. Associate Editor: Ismail Celik.

discussed, supported with some illustrations. The paper closes with a brief outline of the potential of VLES based on transient RANS (T-RANS) to applications in flows featured by strong, quasi-deterministic, large-scale structures. The potential of T-RANS is illustrated in “ultra-hard” (very high Ra number) Rayleigh-Bénard convection, which is inaccessible to the conventional LES, with indication of its possible use to solve large-scale real-life engineering and environmental problems.

## A Perspective on RANS and its Future Role

Currently, an industrial user is confronted with a very broad palette of the available RANS models. The CFD vendors make the choice more difficult by offering in some cases over 20 different RANS variants, with hardly any suggestions in regard to which models should be used for which application. This is not a happy situation and, paradoxically, despite the obvious need for innovation, there seems to be not much incentive for fundamental research in the conventional RANS modeling. Only a few groups over the globe are seriously engaged in RANS research. Furthermore, because of saturation and earlier numerous disappointments, the novelties are today usually met with distrust among both the CFD vendors and CFD users. In contrast, there seems to be much more activity in researching new approaches, primarily in academia, some seemingly departing from the traditional RANS strategies, in search of better physical justification and expanding the range of model applicability. Among such new developments we can identify the following:

- Unsteady RANS (U-RANS) implying time-solution of the conventional RANS for 3D unsteady problems, with or without special treatment of flow unsteadiness
- Multi-scale RANS (one-point and spectral closures)
- Transient RANS (based on conditional or ensemble averaging of NS equations) with possibly modified RANS model for the subscale (unresolved) motion [1]
- VLES based on T-RANS [1], semi-deterministic modeling (SDM) [2], coherent vortex simulation (CVS) [3], partially averaged NS (PANS) [4], and others
- Hybrid RANS/LES with zonal or seamless coupling of the two strategies [5,6]

It is noted that in most of the approaches one deals with the same form of the momentum and scalar transport equation, of course with different meaning of the variables:

$$\frac{D\langle U_i \rangle}{Dt} = \langle F_i \rangle - \frac{1}{\rho} \frac{\partial \langle P \rangle}{\partial x_i} + \frac{\partial}{\partial x_j} \left( \nu \frac{\partial \langle U_i \rangle}{\partial x_j} - \tau_{ij} \right) \quad (1)$$

$$\frac{D\langle T \rangle}{Dt} = \frac{\langle q \rangle}{\rho c_p} + \frac{\partial}{\partial x_j} \left( \alpha \frac{\partial \langle T \rangle}{\partial x_j} - \tau_{\theta i} \right) \quad (2)$$

where  $\langle \rangle$  denotes Reynolds (time or ensemble) averaged quantities in RANS, and filtered quantities in LES, and  $\tau_{ij}$  and  $\tau_{\theta i}$  are turbulent stress and scalar flux, respectively, either for the whole turbulence spectrum (RANS) or its parts (multi-scale RANS), or for unresolved motion (VLES, LES), which in all approaches need to be modeled. The identical forms of Eqs. (1) and (2) for RANS, VLES, and LES make it convenient not only to use the same computational code and similar numerics, but also to combine the two approaches in zonal or hybrid procedure.

A common feature of all these approaches is the desire to capture some elements of the turbulence spectrum, i.e., to resolve in time and space parts—primarily at large scales—of the unsteady turbulent motion. In most methods the focus is on large, dominating eddy structure (beyond, e.g., vortex shedding that can be captured even with the conventional U-RANS) that preserves some coherence and determinism even if the flow is not separated and is steady in the mean. However, because such approaches require a considerable portion of the turbulence spectrum to be modeled (much larger than the conventional subgrid-scale motion in LES),

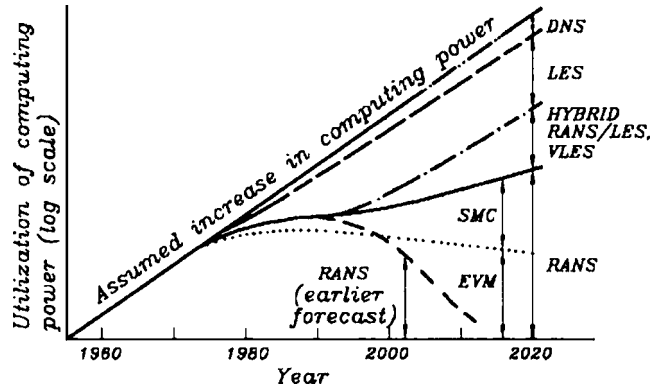


Fig. 1 A conjectured prospect on utilization of the available computing power by different computational approaches

the modeling remains an important issue, which draws to a larger or lesser extent to the RANS experience and makes use of elements of the RANS modeling. This in turn brings new demands and new constraints on RANS models, providing a new incentive for their research.

Putting aside these new developments where RANS models in their original or modified forms will take a new role as “subscale” models (in contrast to subgrid-scale in LES), the fact remains that despite disappointments, we have seen no decline in the use of the conventional RANS models among industry. It is conjectured that this trend will remain for a foreseeable future, more or less in line with the increase in the computing power, because of

- increasing market pressure to shorten the design and marketing time, putting higher demands on faster parametrization and design optimization
- increasing improvement and wider (and less expensive) availability of the commercial CFD codes, easier and user-friendly grid-generation, and postprocessing (visualization and animation) software
- expanding the number of CFD users among medium and small industries
- broadening of the applicability of CFD and the increasing needs to handle more and more complex industrial problems involving heat and mass transfer, combustion and other chemical reactions, multi phases, etc., where prohibitive demands on computer resources and uncertainties in modeling physical phenomena other than turbulence make little incentive to use sophisticated turbulence models and LES.

Pope [7] also argues that most of the increase in the computer power will in the near future be used for RANS, aimed at improving spatial resolution and better numerical accuracy by using larger and better designed numerical meshes and more accurate representation of geometry and its boundaries, as well as using more sophisticated models of turbulence and other phenomena. We can also expect more use of U-RANS for 3D computations of complete bluff bodies to capture better unsteady separation effects. Also, visualization and animation, which usually requires large computing power, will be more and more in use as a tool for identifying some global or local flow features that can help in improving design.

A conjecture on possible future utilization of the increased computing power is presented in Fig. 1. Of course, the proportion of LES (and DNS) will be much smaller among the industrial users, whereas the opposite can be expected in research communities.

## LES Niches for Heat Transfer

For accurate predictions of wall bounded flows, especially if wall phenomena—friction, heat and mass transfer—are in focus,

LES is severely constrained by the near-wall resolution requirements. Proper resolution of the near-wall streaky structures requires grid density close to that for DNS with near-wall grid spacing not larger than  $\Delta y^+ = O(1)$ ,  $\Delta x^+ = O(50)$ , and  $\Delta z^+ = O(20)$ , where  $y^+$  denotes the wall-normal,  $x^+$  streamwise, and  $z^+$  spanwise direction in wall units. As Re and Ra numbers increase, the molecular sublayers becomes progressively thinner, imposing formidable demand on grid fineness. Handling complex wall topology is another problem with LES, because a rational boundary fitting requires an unstructured grid which is still not widely tested for LES.

Yet, there are many flows and heat transfer problems of practical relevance where the Re or Ra numbers are relatively low and where LES can be very suitable, reliable, and even the indispensable technique. Currently actual examples are electronics cooling, internal cooling of gas turbine blades, crystal growth, and others. While RANS models can also give useful results, the ever-increasing trends toward miniaturization and hence higher specific heat dissipation in electronics cooling, or higher heat fluxes in internal passages of high-load gas turbine blades, bring in focus the problem of hot spots and thermal fatigue, which require accurate prediction of temperature distribution and its time variation. This is illustrated in an example where LES in conjunction with an unstructured solver has been applied for conjugate flow and heat transfer over a multi-layered wall-mounted protrusion imitating an electronic component. Apart from the cubical shape, chosen on purpose to serve as a reference for investigating conjugate heat transfer, all other aspects correspond to real electronics element: a copper core of 13.5 mm cube heated electrically simulates the heat dissipation, whereas the low-conducting 1.5 mm thick epoxy layer on the cube surface mimics the real coating. Because of low conducting surface layer, the surface temperature is highly nonuniform and—depending on the local flow and turbulence structure—locally it may exceed the technological limits (local hot spots) and cause equipment malfunctioning. The time-averaged temperature distribution over the surface can easily be measured (liquid crystals, infrared camera, thermocouples, etc.) but capturing well-resolved instantaneous temperature field is almost impossible with the available techniques because of high frequencies of the fluctuations. Well-resolved LES or DNS appear to be the only route to predict accurately the time variation of the surface temperature distribution.

An example of such simulations can be found in Niceno et al. [8] where LES of flow and conduction in the epoxy layer have been solved simultaneously. Filtered momentum and energy equations (1) and (2) were closed by  $\tau_{ij} = 2\nu_{sgs}\langle S_{ij} \rangle$  and  $\tau_{\theta i} = (\nu_{sgs}/Pr)\langle \partial T/\partial x_i \rangle$  and solved on an unstructured grid. Because near the cube walls the grid is sufficiently fine to approach DNS, the choice of the subgrid scale model is not influential. Thus, the standard Smagorinski subgrid-scale model was used with  $\nu_{sgs} = (C_s\Delta)^2(2\langle S_{ij}S_{ij} \rangle)^{1/2}$  where  $\Delta = \min(d, \Delta V^{1/3})$ ,  $C_s = 0.1$ , and  $d$  is the distance from the nearest wall.

Comparison of various computed properties with experiments of Meinders and Hanjalic [9] are reported in detail in [8], showing generally very good agreement. It is noted that the time-averaged temperature shows a strong variation over the cube surface, dropping from maximum of 60°C at the rear surface to 40°C at the intensively cooled front edges (note that the copper core was at 75°C) [8]. This surface temperature nonuniformity was found to reflect a range of vortex structures, which are difficult to capture by any RANS model.

Especially useful results from the LES are the *instantaneous* temperature imprints on the cube surfaces, which cannot be obtained by any other technique, experimental or numerical, except by DNS. The simulations show high local temperature nonuniformities with a pattern changing continuously with a stochastic periodicity, as can be observed from the surface temperature animation. Figure 2 shows one realization of the instantaneous surface temperature viewed from the front and rear side. Local hot spots

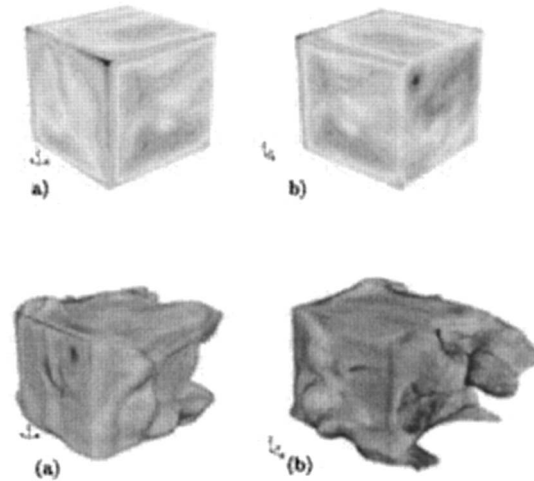


**Fig. 2** Instantaneous temperature on the cube surface (above) and thermal plumes around the cube, defined by the isosurface of  $T = 24.5^\circ\text{C}$  (below). (a) view from the front, (b) view from the back. The flow is in the  $x$  direction [8].

are discernible on the rear face. The instantaneous fluid temperature corresponding to the same realizations is also shown in the form of thermal plumes defined by the surface of constant temperature of  $24.5^\circ\text{C}$  and colored by fluid velocity magnitude.

### Some Recent Developments in RANS

Limitations of linear eddy viscosity models (EVMs) have been recognized already in the early days of turbulence modeling and the attention has been turned to the second moment closure (SMC) that makes the most logical and physically most appropriate RANS modeling framework. This approach requires modeling and solution of the transport equations for the turbulent stress and scalar flux:

$$\frac{D\overline{u_i u_j}}{Dt} - D_{ij} = \overline{(f_i u_j + f_j u_i)} - \left( \overline{u_i u_k} \frac{\partial U_j}{\partial x_k} + \overline{u_j u_k} \frac{\partial U_i}{\partial x_k} \right) + \phi_{ij} - \varepsilon_{ij} \quad (3)$$

$$\frac{D\overline{\theta u_i}}{Dt} - D_{\theta i} = -\overline{u_i u_j} \frac{\partial T}{\partial x_j} - \overline{\theta u_j} \frac{\partial U_i}{\partial x_j} - \overline{f_i \theta} - \varepsilon_{\theta i} + \phi_{\theta i} \quad (4)$$

which are closed by a scale-providing equation, usually energy dissipation rate  $\varepsilon$  or  $\omega = \varepsilon/k$ . This level of modeling enables the exact treatment of the turbulence production by the mean strain or body forces. Furthermore, the solution of transport equations for each stress component makes it possible—at least in principle—to reproduce accurately the stress field and its anisotropy, which reflects the structure and orientation of the stress-bearing turbulent eddies. This in turn makes it possible to reproduce effects of streamline curvature, rotation and swirl, secondary motion, and other effects encountered in complex flows, better than with an eddy-viscosity concept [10].

Despite obvious advantages, two issues emerged immediately as critical: modeling, especially of the pressure-strain terms  $\varphi_{ij}$  and  $\varphi_{\theta i}$ , and the numerical stiffness of the coupling of Eqs. (3) and (4) with the mean momentum and energy equations. While the modeling has been reasonably successful with some notable improvements over the past few years, the numerical stiffness and the reluctance of users to solve more differential equations remained long the major deterrent. Over the years it became clear that the numerical problem has been associated primarily with the tendency to use the available Navier-Stokes solver designed for equations with dominant diffusive second-order term pertinent to eddy viscosity approach. Providing turbulent stresses and fluxes

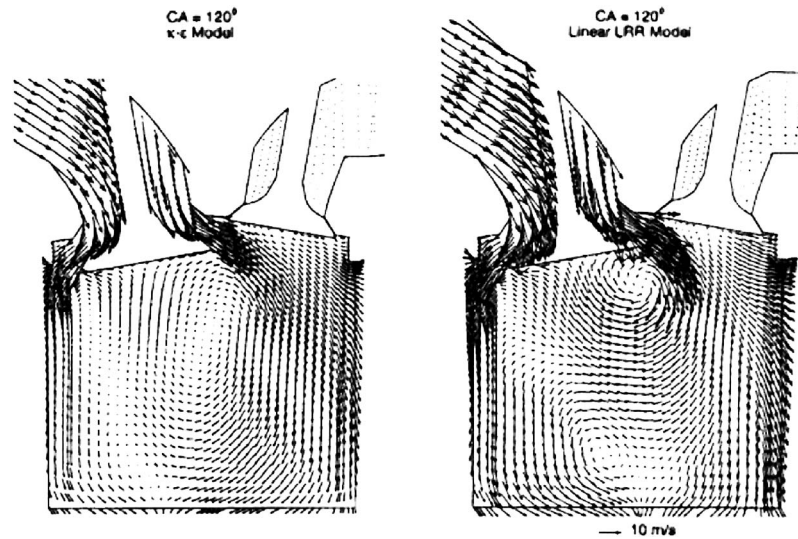


Fig. 3 Velocity vectors in the midplane of a DOHC IC engine at CA=120°, 3D RANS [18]. Left:  $k-\epsilon$ ; right: SMC.

from separate differential equations requires more care in coupling the equations. This was demonstrated recently by Gerolymos et al. [11], who, thanks to an efficient implicit implementation of the second-moment closure, succeeded in computing several complex turbomachinery flows with a near-wall second-moment closure with only 30% more computing time than required for the  $k-\epsilon$  model. Over the past decade a number of groups, both in industry and academia (Craft and Launder at UMIST, e.g., [12], Leschziner et al. at Imperial College [13], Basara et al. AVL, Graz, Austria [14,15], Gerolymos et al. at Univ. Pierre-et-Marie Curie in Paris, [11,16], Yang et al. at Michigan Tech., Houghton, USA [17,18], to name only a few), succeeded in designing similar or other remedies that make the solution of the second-moment closure almost a routine procedure that requires only marginally larger effort and computing resources as compared with the EVMs. The improvements, however, in most cases appeared to be worth the effort. A number of examples illustrating the superiority of the second-moment closure can be found in the above cited and other references. A good selection of complex industrial flows, solved in parallel with the  $k-\epsilon$  and the SMC models (all with wall functions) using KIVA code, can be found in Refs. [17,18], these include a nonreacting multi-point lean direct injection (LDI) gas turbine combustor with discrete jet- and helical axial swirlers of different orientations, a simplified direct injection stratified charged (DISC) IC engine, a lean-premixed pre-vaporized (LPP) combustor, and a four-valve double-overhead camshaft (DOHC) IC engine. In all cases, the predictions with the SMC with the Speziale, Sarkar and Gatski (SSG) [19] pressure-strain model appeared in better agreement with experiments (where available) than the standard  $k-\epsilon$ . In cases where no experimental data for field properties were available, the integral parameters were compared, showing again better agreement with the SMC. For example, for the DOHC engine the experimentally observed strong swirl generated by the canted valves and the piston motion at CA approaching 180° was much better reproduced by the SMC (Fig. 3). While there is still room for improvement, these and other examples serve as good illustrations of the current achievements in solving complex flows of industrial relevance with the second-moment closure.

Second-moment closures have also served as inspiration for a number of improvements of lower-order models. Algebraic stress and flux models based on their differential parent equations—in

implicit or explicit forms—have been found to perform generally better than the nonlinear eddy viscosity models that were derived independently, e.g., Wallin and Johanson [20].

The elliptic relaxation EVM of Durbin [21] was also inspired and derived with resource to the model differential stress equation (3). A broad variety of nonlinear eddy-viscosity models, developed for the desire of industry with the hope to become a more user-friendly surrogate for second-moment closure, have generally not fulfilled their promises. Some of the rigorously derived models that were relatively free from arbitrary tuning of numerous coefficients, such as the TCL (two-component limit) cubic model of Craft et al. [22], were reported to perform well in several flows considered, though less satisfactory in some other flows, e.g., [23]. However, because of their complexity, the more successful (but, as a rule, more complex) nonlinear models have not yet appealed to industry.

In view of the above discussion, it is fair to say that the RANS models are witnessing their renaissance and that we shall see in the near future more extensive use of advanced RANS models applied to complex flows.

We consider briefly some recent advancements, aimed at robust application of advanced models to complex flows. Recently reported novelties are too numerous for this brief coverage and we will restrict the discussion to only a few developments originating from the author's group.

**Robust Elliptic Relaxation EVMs.** The  $v^2$ - $f$  model of Durbin [20] appeared as an interesting novelty in engineering turbulence modeling. By introducing an additional (“wall-normal”) velocity scale  $v^2$  and an elliptic relaxation concept to sensitize  $v^2$  to the inviscid wall blocking effect, the model dispenses with the conventional practice of introducing empirical damping functions. Because of its physical rationale and of its simplicity, it is gaining in popularity and appeal especially among industrial users. While in complex three-dimensional flows, with strong secondary circulation, rotation, and swirl, where the evolution of the complete stress field may be essential for proper reproduction of flow features, the model remains still inferior to the full second-moment and advanced nonlinear eddy viscosity models, it is certainly a much better option than the conventional near-wall  $k-\epsilon$ ,  $k-\omega$ , and similar models.

However, the original  $v^2$ - $f$  model possesses some features that

impair its computational efficiencies. The main problem is with the wall boundary condition  $f_w \rightarrow -20v^2\nu^2/(\varepsilon y^4)$  when  $y \rightarrow 0$ , which makes the computations sensitive to the near-wall grid clustering and—contrary to most other near-wall models—does not tolerate too small  $y^+$  for the first near-wall grid point. The problem can be obviated by solving simultaneously the  $v^2$  and  $f$  equation, but most commercial as well as in-house codes use more convenient segregated solvers. Alternative formulations of the  $v^2$  and  $f$  equations that permit  $f_w=0$  usually perform less satisfactorily than the original model and require some retuning of the coefficients.

Recently a version of the eddy-viscosity model based on Durbin's elliptic relaxation concept has been proposed [24], which solves a transport equation for the velocity scale ratio  $\zeta=v^2/k$  instead of the equation for  $v^2$ ,

$$\frac{D\zeta}{Dt} = f - \frac{\zeta}{k}P + \frac{\partial}{\partial x_j} \left[ \left( \nu + \frac{\nu_t}{\sigma_\zeta} \right) \frac{\partial \zeta}{\partial x_j} \right] \quad (5)$$

in combination with an elliptic relaxation function (here based on the SSG [19] quasi-linear pressure-strain model)

$$L^2 \nabla^2 f - f = \frac{1}{\tau} \left( c_1 + C_2 \frac{P}{\varepsilon} \right) \left( \zeta - \frac{2}{3} \right) \quad (6)$$

Here the eddy viscosity is defined as  $\nu_t = c_\mu \zeta k \tau$ , where  $c_\mu$  is different from the conventional  $C_\mu$ , and  $\tau$  is the time scale, equal to  $k/\varepsilon$  away from a wall. Because of a more convenient formulation of the equation for  $\zeta$  and especially of the wall boundary condition for the elliptic function  $f_w = -2\nu\zeta/y^2$ , this model is more robust and less sensitive to nonuniformities and clustering of the computational grid. Alternatively, one can solve Eq. (6) for a "homogeneous" function  $f'$  with zero wall boundary conditions  $f'_w=0$ , and then obtain  $f=f' - 2\nu(\partial\zeta^{1/2}/\partial x_n)^2$  (in analogy with Jones-Launder equation for homogeneous dissipation). The computations of flow and heat transfer in a plane channel, behind a backward-facing step and in a round impinging jet, show in all cases satisfactory agreement with experiments and direct numerical simulations [24].

**Elliptic-Blending SMC.** As an example of a robust second-moment closure suitable for complex near-wall flows, we discuss briefly the elliptic blending model (EBM) of Manceau and Hanjalić [25]. The model, based on Durbin's [26] SMC, solves Eq. (3) in conjunction with the  $\varepsilon$  equation, but instead of solving six elliptic relaxation equations for the functions corresponding to each stress component, a single scalar elliptic equation is solved:

$$\alpha - L^2 \nabla^2 \alpha = 1 \quad (7)$$

The pressure strain term and the stress dissipation are modeled by blending the "homogeneous" (away from the wall) and the near-wall models

$$\phi_{ij} = (1 - \alpha^2) \phi_{ij}^w + \alpha^2 \phi_{ij}^h \quad (8)$$

$$\varepsilon_{ij} = (1 - \alpha^2) \frac{u_i u_j}{k} \varepsilon + \frac{2}{3} \alpha^2 \varepsilon \delta_{ij} \quad (9)$$

In Eq. (8),  $\phi_{ij}^h$  can be chosen from any known model (we use SSG), whereas the wall model for the pressure strain, satisfying the exact wall limit and stress budget, is defined by

$$\phi_{ij}^w = -5 \frac{\varepsilon}{k} \left( \overline{u_i u_k n_j n_k} + \overline{u_j u_k n_i n_k} - \frac{1}{2} \overline{u_k u_l n_k n_l} (\overline{n_i n_j} + \delta_{ij}) \right) \quad (10)$$

where the unit wall-normal vector is evaluated from

$$\mathbf{n} = \frac{\nabla \alpha}{\|\nabla \alpha\|} \quad (11)$$

**Illustration of the EBM in Multiple-Impinging Jets.** As an illustration of the performance of the EBM, we show some results of computations of flow and heat transfer in a multiple impinging

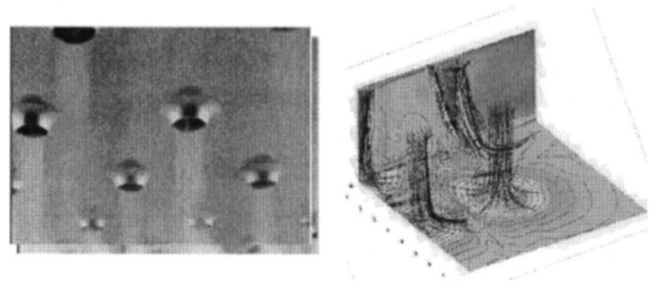


Fig. 4 Nozzle configuration and computational view of streamlines and surface temperature

jets configuration, shown in Fig. 4 [27,28]. Besides its relevance for cooling, heating, and drying in various applications, impinging jets have long served as a generic benchmark for turbulence and heat transfer modeling.

In the wall layer in an impinging jet, the turbulent stress tensor shows high anisotropy which is reflected in the turbulent heat flux anisotropy and, in turn, in the local wall heat transfer. The wall-normal heat flux wall is governed primarily by the wall-normal velocity fluctuation. The change of flow direction from a normally impinging jet to a radial wall jet causes a strong redistribution between the stress component, as well as a change of the roles of different components of the mean velocity gradient from one region to another. This leads to a strong evolution of stress and heat flux anisotropy and to a change in the intensity and the role of the wall-normal stress component. Because most linear eddy-viscosity models cannot reproduce properly the stress anisotropy, they fail in reproducing heat transfer. That the stress field is closely related to heat transfer can be illustrated also indirectly: the models which reproduce well the turbulence stress field yield as a rule better predictions of wall heat transfer, even if a simple eddy-diffusivity concept is used for the turbulent heat flux.

Multiple-impinging jets are more complex. Possible jet interaction prior to impingement and the collision of wall jets on the target plate create complex 3D patterns with ejection fountain, recirculation, and embedded vortices in the space between the jets, as well as a cross flow towards escape openings. The arrangement and spacing of the jets have crucial roles in achieving optimum effects. Instantaneous PIV shows that closely spaced jets only intermittently reach the impinging surface with full strength [29]. Curious phenomena, such as symmetry breaking, have been observed in some arrangement affecting heat transfer uniformity. Reliable computational optimization is essential for reaching the optimum effects and, because of flow complexity, sophisticated models are required to trust the computations. Wall functions are unreliable and equations must be integrated up to the wall.

We present some results for a square arrangement of nine equal parallel jets issuing from the same orifices, with three models: the conventional  $k-\varepsilon+WF$ , the  $v^2-f$ , and the EBM, compared with experiments. The EBM has been used in conjunction with two different heat flux models, i.e., the isotropic and nonisotropic eddy diffusivity models (known also as simple and generalized gradient diffusion hypotheses, SGDHD and GGDH, respectively):

$$\text{SGDH: } \overline{\theta u_i} = - \frac{\nu_t}{\sigma_T} \frac{\partial T}{\partial x_i}; \quad \text{GGDH: } \overline{\theta u_i} = - C_\theta \frac{k}{\varepsilon} \frac{\partial T}{\partial x_j} \frac{\partial u_j}{\partial x_i}$$

All models indicate that the jets do not interact much prior to the impingement and a void space appears in between where a trapped low-momentum vortex resides asymmetrically displaced above the 45° symmetry line, as shown in Figs. 5 and 6. This broken symmetry, despite fully symmetric stationary conditions imposed on both interior vertical and horizontal symmetry planes of the solution domain, is also confirmed by experiments [29] as shown in the figures.

The predictions of the flow pattern and Nusselt (Nu) number

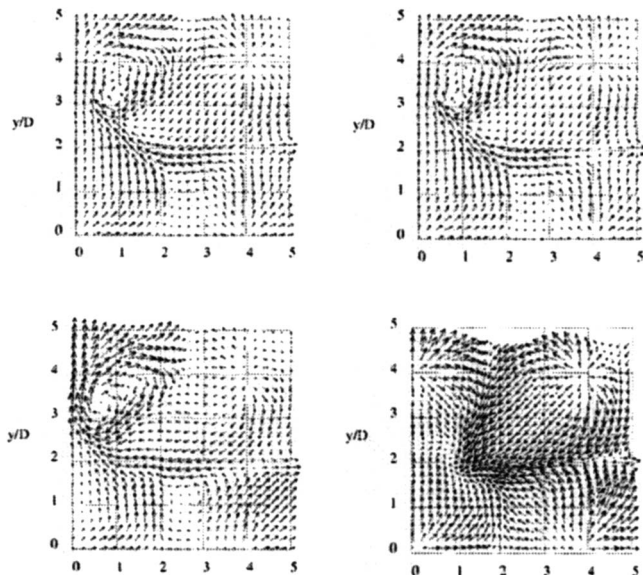


Fig. 5 Velocity vectors in a plane at  $z/D=0.54$  above the impinging plane. Top:  $k-\epsilon+WF$  (left), EBM (right); bottom:  $k-v2-f$  (left), PIV measurements (right) [28].

with different models differ significantly. Unlike in single jets, where the  $k-\epsilon$  model predicts maximum Nu number in the stagnation region, here it shows notable underprediction. In contrast, the  $v^2-f$  returns higher Nu, somewhat in better agreement with experiments, but still unsatisfactory. The EBM second-moment closure shows surprisingly good reproduction of details of the flow pattern in the whole domain and excellent predictions of Nusselt number, as shown also in Fig. 7, where the effect of the heat flux model is also illustrated.

**Multiple-Scale RANS.** Another niche where we may see more activity in the near future are the two-scale or multi-scale RANS models in which additional scalar equations are solved to provide

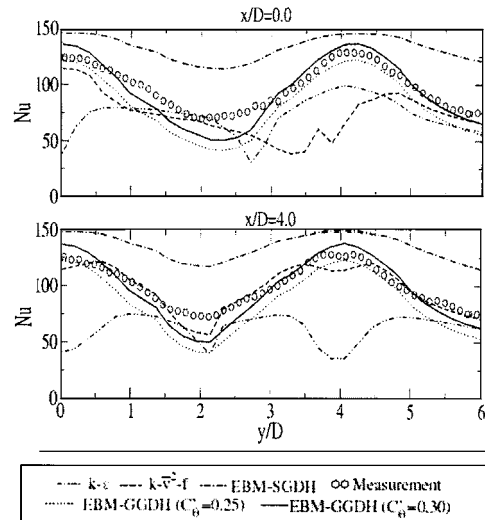


Fig. 7 Nusselt number distribution across the jets centerlines for two locations [28]

extra turbulence scales. The usage of a single turbulence time and length scale to characterize all processes and to model undefined terms in the governing equations has long been recognized as one of the major deficiencies of the conventional RANS. Early attempts based on a split spectrum method [30,31], where a set of model equations was derived and solved for each of the two (or more) spectrum slices, seemed promising but the development was discouraged by the lack of information on spectral splitting in complex flows and by the inevitable increase in the number of empirical coefficients (a separate set needed for each spectrum slice). Some developments following different rationale have been reported recently, aimed primarily at deriving an equation for an additional turbulence scale to distinguish the spectral energy transfer from the turbulence dissipation rate. Such a model, based on the weighted integration of the dynamic equation for the cova-

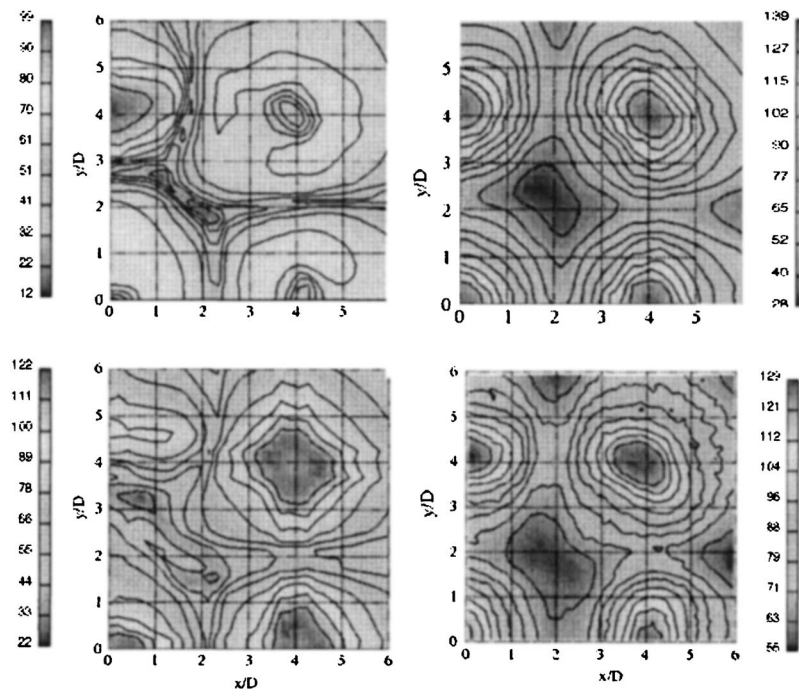


Fig. 6 Nusselt number predicted by different models. Top:  $k-\epsilon+WF$  (left), EBM+GGDH (right); bottom:  $k-v2-f$  (left), LCT measurements (right) [28].

riance spectrum, with an assumed shape of the energy spectrum and spectral anisotropy function, has been considered by Cadiou et al. [32]. With some simplification, separate equations are derived for the spectral energy transfer function  $\varepsilon_p$  and the true dissipation rate  $\varepsilon$ , which in spectral equilibrium become equal. Tests in several nonequilibrium flows, which include a periodically perturbed flow over a backward-facing step and over a square-section rod, showed interesting dynamics of the two time scales, defined as  $k/\varepsilon_p$  and  $k/\varepsilon$  [32].

### Hybrid RANS/LES

It is recalled that the proper resolution of dynamically important scales with LES requires the grid density to increase with  $Re^{0.4}$  in regions away from a solid wall, but this constraint becomes much more severe in near-wall regions where the grid density should follow  $Re^{1.8}$ . In contrast, the RANS grid requires clustering only in the wall-normal direction, making the grid requirements proportional to  $\ln(Re)$ . For realistic engineering and environmental flows an attractive proposition is to combine the LES with RANS strategy. Most approaches currently under exploration can be grouped into two categories. The first is the zonal approach in which the conventional coarse-grid LES is applied in one flow region, usually away from a solid wall, and a RANS model is applied in the other, usually the near-wall region. The switching from one to another field is made at a suitably chosen interface. The key problem is to ensure proper matching conditions at the interface, which are usually based on the equality of the total (resolved+modeled) stress or total viscosity. Because the resolved motion on both sides of the interface should be the same, and RANS model yields a much larger modeled contribution than the LES subgrid-scale model, the RANS model needs to be damped. A way to accomplish matching is to damp the RANS eddy viscosity either by damping the eddy-viscosity coefficient  $C_\mu$  [33] or by decreasing the RANS kinetic energy or by increasing the dissipation rate [34]. Other approaches have also been reported, e.g., a parabolic treatment of the near-wall boundary layer with imbedded solutions using a simple damped mixing length model in the near-wall RANS region, or the simultaneous solution of the parabolic momentum equation—again with mixing length, with LES in the outer region.

The second approach is based on continuous (nonzonal) simulations using the same model for the unresolved motion in the complete solution domain, which serves as a RANS model in the near-wall region and as a subgrid-scale model in the outer LES region. The switching between one and the other approach is accomplished by changing the length scale: in the near-wall RANS region the distance from the wall is used whereas in the LES region this is replaced by the representative grid size. The most known method in this category is Spalart's detached eddy simulation (DES) [35] in which the Spalart-Almaras (S-A) one-equation model for eddy viscosity is used in both regions. This approach, just like the zonal one, contains a dose of arbitrariness: the interface between the RANS and LES region is determined by the adopted mesh. The switching parameter can of course be adjusted by an empirical coefficient, but the desired criterion is difficult to know in advance in unknown complex flows. The problem is in the strong deterioration of the predictions when the switching occurs at larger distances from the wall ( $y^+ > 30$ ). It is also noted that the S-A model was tuned for external aerodynamic flows and has been shown to perform badly in some other flow types.

The zonal approach seems more appealing because outside the wall boundary layers, the conventional LES method [with prescribed sub-grid-scale (sgs) or dynamic modeling] is used without any intervention in the subgrid modeling. However, the crucial issues and problems to address are the location and the definition of the interface, the nature of matching conditions, especially for flows in complex geometries, and the receptivity of the RANS region to the LES unsteadiness and the RANS feedback into the

LES region. Even if the RANS model is adjusted to meet the constraint of continuity of eddy viscosity and other quantities across the interface, an insufficient level in small-scale activity that RANS feeds into LES across the interface produces in most circumstances nonphysical features (a bump) in the velocity profile around the interface. Several proposals have been published for introducing an extra small-scale forcing. Piomelli et al. [36] suggested a "stochastic backscatter" generated by random number with an envelope dependent on the wall distance. Davidson and Dahlström [37] proposed to add turbulent fluctuations, obtained from DNS of a generic boundary layer, to the momentum equation at the LES side of interface. Hanjalic et al. [6,33] found that by feeding the instantaneous instead of homogeneously averaged value of  $C_\mu$  at the interface (that matches the RANS eddy viscosity with the subgrid-scale viscosity on the LES side) the anomaly diminishes. This suggests that the "noisy" instantaneous  $C_\mu$  acts in a similar spirit as the additional random or stochastic forcing, but it is much simpler.

Defining the criteria for the positioning of the interface is another problem. The kink in the velocity profile seems most visible if the interface is placed in the region populated by coherent streaks (centered around  $y^+ = 60-100$ ). Because of insufficient spanwise grid spacing, the computed streaks are much wider ("superstreaks") and their distance much larger than in reality. Moving the interface closer to the wall would lead to a greater proportion of the small-scale structure being captured, but reproducing faithfully the streak topology would require the grid to be substantially refined, especially in the spanwise direction, thus departing from the main motivation for the hybrid approach. On the other hand, moving the interface further away from the wall leads to the streaky pattern becoming progressively indistinct.

Paradoxically, with the interface placed at a distance sufficiently large to lose the fine near-wall structure, the anomaly in the velocity profile gradually disappears. This finding may sound discomforting on theoretical grounds, but has comforting implications in the simulation of complex flows at very high Re numbers, where the wall boundary layers are in any case so thin that they cannot be resolved in any event.

The above arguments call, however, for more advanced RANS models to be used in the near-wall RANS regions. An example of such an approach is the combination of an elliptic relaxation EVM ( $v^2$ -f or  $\zeta$ -f) model for RANS with the dynamic sgs for LES [38]. The dissipation rate in the  $k$  equation is multiplied by a function in terms of the RANS and LES length scale ratio, i.e.,

$$\frac{Dk}{Dt} = \frac{\partial}{\partial x_j} \left( (\nu + \nu_t) \frac{\partial k}{\partial x_j} \right) + P - \xi \varepsilon \quad (12)$$

where

$$\xi = \max \left( 1, \frac{L_{RANS}}{L_{LES}} \right); \quad L_{RANS} = \frac{k_{tot}^{3/2}}{\varepsilon}; \quad L_{LES} = 0.8(\Delta x \Delta y \Delta z)^{1/3}$$

and  $k_{tot} = k_{res} + k_{mod}$ . Hence, for  $L_{RANS} < L_{LES}$ , the RANS model is in play, and for  $\xi > 1$  we should have a dynamic LES. In order to avoid a discontinuity at the interface when  $\xi = 1$ , a "buffer" zone is introduced where RANS is still in play but with an automatic adjustment (through  $\xi > 1$ ) in the RANS eddy viscosity to the LES sgs dynamic viscosity. In examples shown below the buffer zone extends up to  $\xi \approx 1.5$ , covering only a few cells for the typical RANS and coarse-LES grids used here.

Figure 8 shows velocity profiles in a plane channel obtained from hybrid computations with the above model for three Reynolds numbers using a RANS-type (coarse) mesh of  $64 \times 64 \times 32$  cells (mesh 1) for  $Re_\tau = 590$  and 2000, and  $64 \times 90 \times 32$  (mesh 2) for  $Re_\tau = 20,000$ . Note that the grids for the two higher  $Re$ 's are two orders of magnitude smaller than required for properly resolved LES. The results are very satisfactory, though the true test must await justification in more complex flows.

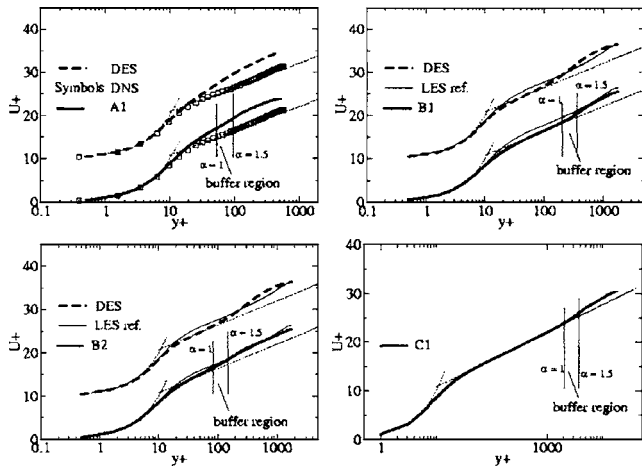


Fig. 8 Hybrid RANS ( $v^2$ - $\bar{\eta}$ )+LES (dynamic sgs) velocity in a plane channel [38]. A, B, and C indicate three different Re numbers, and 1 and 2 indicate two different grids.

### T-RANS-Based VLES

Methods that combine RANS and LES strategy can generally be classified as very-large eddy simulations (VLESS). The name implies a form of LES (not necessarily based on grid-size filtering) with a cutoff filter at a much lower wave number, or simply solving ensemble averaged equations. The basic rationale behind VLES is resolve only very large, coherent, or deterministic structures and model the rest! Modeling a larger part of the spectrum requires a more sophisticated model than the standard sub-grid-scale model for LES, i.e., a form of RANS model that is not related to the size of the numerical mesh. As compared with the conventional RANS, the model is required only for the incoherent random fluctuations, while the large scales are resolved. The solution of the resolved part of the spectrum can follow the traditional LES practice using grid size as a basis for defining the filter (hence the name hybrid RANS/LES), or solve ensemble-or conditionally averaged Navier-Stokes equations.

We present here briefly some features and illustrations of the latter approach, named T-RANS (transient RANS) [39,40] and demonstrate its application to confined turbulent flows subjected to thermal buoyancy. It is recalled that an instantaneous flow can be decomposed into unsteady ensemble-averaged (organized) motion and random (incoherent) fluctuations, so that the instantaneous flow property  $\hat{\Psi}(x_i, t)$  can be written as the sum of time-mean, deterministic, and random parts. The ensemble averaged (mean plus deterministic) quantities are fully resolved by solving in time and space equations (1) and (2)—just as in LES, whereas the unresolved contribution is modeled using RANS models for instantaneous stress and scalar flux. The total long-term averaged second moments consist of the resolved (deterministic) and incoherent (random) part which are assumed not to interact, i.e.,  $\hat{\Psi}\hat{\Psi} = \bar{\Psi}\bar{\Psi} + \hat{\Psi}\hat{\Psi} + \overline{\varphi\gamma} = \langle \hat{\Psi} \rangle \langle \hat{\Psi} \rangle + \overline{\varphi\gamma}$ . Both parts are expected to be of the same order of magnitude, with the modeled contribution prevailing in the near-wall regions where the deterministic motion is weak. The dominance of the modeled contribution in the near-wall region emphasizes the importance of the RANS model which needs to be well tuned to capture near-wall behavior of turbulent stress and scalar flux.

We illustrate the potential of T-RANS in the example of Rayleigh-Bénard convection at extreme Rayleigh numbers, which are inaccessible to either conventional LES (or DNS) or to classic RANS. Here we use the algebraic subscale flux model and the corresponding algebraic stress model in which all variables are evaluated as time dependent [39,40]. Extensive testing of the RANS subscale model in a number of confined natural convection

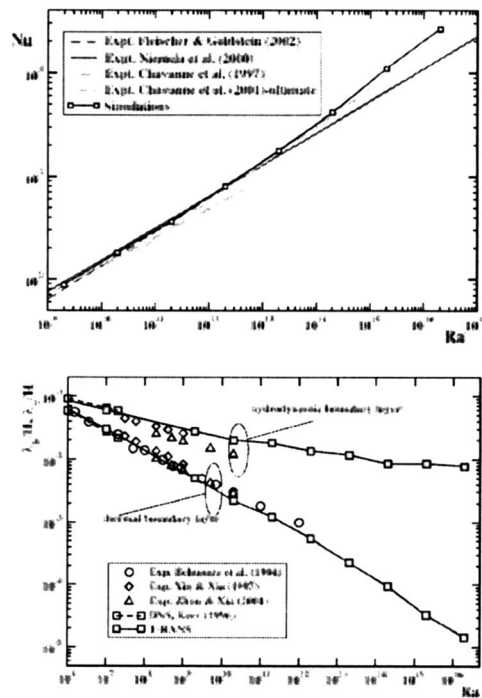


Fig. 9 T-RANS predictions of Nu number (above) and of hydrodynamic ( $\lambda_v$ ) and thermal ( $\lambda_\theta$ ) wall layer thickness (below) in R-B convection over ten decades of Ra number [40]

cases provides confidence in its performance close to walls. Outside the wall layers, the role of the model fades away because the dominant large-scale quasi-deterministic roll structures are fully resolved in time and space.

Figure 9 shows T-RANS computations of the Nusselt number and of the hydrodynamic ( $\lambda_v$ ) and thermal ( $\lambda_\theta$ ) wall layer thickness (defined by peak positions of the turbulent kinetic energy and temperature variance, respectively) as a function of Rayleigh number over ten decades, up to  $10^{16}$  [40]. It is noted that the maximum Ra achievable by DNS is around  $10^8$  and by true LES about  $10^9$ . The T-RANS computations agree very well with the available DNS for low Ra numbers as well with the experiments for low and moderate Ra (up to  $10^{12}$ ) in accord with the known correlations  $Nu \propto Ra^{0.3}$ ,  $\lambda_v/H \propto Ra^{-1/7}$  and  $\lambda_\theta/H \propto Ra^{-1/3}$ .

For higher Ra numbers the T-RANS shows clearly an increase in the exponent of Ra in accord with Kraichnan's asymptotic theory ( $n \rightarrow 0.5$  for  $Ra \rightarrow \infty$ ) and recent experiments. This change in Nu-Ra slope is reflected in the change of the slopes of  $\lambda_v(Ra)$  and  $\lambda_\theta(Ra)$  curves. The capability of T-RANS for capturing the instantaneous structures is illustrated in Fig. 10, where instantaneous streaklines are presented for the central and a near-wall

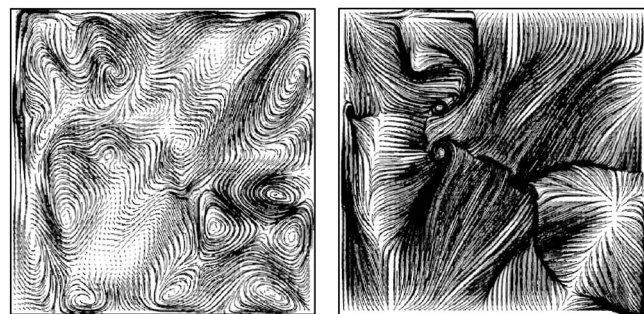


Fig. 10 T-RANS instantaneous trajectories in R-B convection for  $Ra=2 \times 10^{14}$  ( $Pr=0.71$ ). Left: at midplane ( $z/H=0.5$ ); right: close to the top wall ( $z/H=0.925$ ) [40].



plane for  $Ra=2 \times 10^{14}$ . The T-RANS method proved subsequently to be very suitable for real engineering and environmental flows and transport phenomena at mezzo scales, e.g., for predicting diurnal change in air flow and pollutant dispersion [41].

## Conclusions

Will RANS methods survive LES? This author believes that they will, at least in the next few decades. True, the anticipated further increase in computing power and wider accessibility of inexpensive high performance computers will certainly breed expanded efforts in the LES and further improvements in LES-specific numerics and subgrid-scale models can be foreseen. Already, we are witnessing LES on meshes with  $O(10^8)$  cells and it is realistic to expect that within a decade such computations would be much more frequent. LES in knowledgeable hands will take an increasingly important role as a research tool in parallel with DNS. But we will probably witness also more LES abuse and false claims: LES is relatively easy to perform provided one has sufficient computing power at one's disposal. And, temptations are great. Conventional LES on a too-coarse grid of wall bounded flows, especially in attached flows regions, can be very erroneous and inferior to even simple conventional RANS.

However, in the view of this writer, it is difficult to imagine that LES will in the foreseeable future replace RANS as a daily design tool. The major impact of the impressive increase in the computing power over the past three decades has been in the shortening of the design cycle and marketing time for new products, but has had little influence on industrial preference for turbulence models. Despite the undisputable progress in the development of advanced models, the rudimentary  $k-\epsilon$  (and, to a less extent,  $k-\omega$ ) model launched 35 years ago serves still as the most frequently used closure. It is realistic that this trend will continue, though hopefully we should expect to see more advanced RANS and U-RANS based on second-moment closure and their hybridization with LES.

## Acknowledgment

The illustration used in this paper originated from the work of my colleagues and students: S. Kenjereš, B. Niceno, L. Tielen, and S. L. Yang.

## References

- Hanjalic, K., and Kenjereš, S., 2001, "T-RANS Simulation of Deterministic Eddy Structure in Flows Driven by Thermal Buoyancy and Lorentz Force," *Flow, Turbul. Combust.*, **66**, pp. 427–451.
- Ha Minh, H., and Kourta, A., 1993, "Semi-Deterministic Turbulence Modeling for Flows Dominated by Strong Organized Structures," *Proc. 9th Int. Symp. on Turb. Shear Flows*, Kyoto, Japan, pp. 10.5-1–10.5.6.
- Farge, M., Schneider, K., Pellegrino, G., Wray, A. A., and Rogallo, R. S., 2003, "Coherent Vortex Extraction in Three-Dimensional Homogeneous Turbulence: Comparison Between CVS-Wavelet and POD-Fourier Decomposition," *Phys. Fluids*, **15**(10), pp. 2886–2896.
- Girimaji, S. S., Srinivasan, R., and Jeong, E., 2003, "PANS Turbulence Model for Seamless Transition Between RANS and LES: Fixed-Point Analysis and Preliminary Results," Paper No. FEDSM2003-45336, Proc. ASME FEDSM'03.
- Spalart, P., 2000, "Strategies for Turbulence Modelling and Simulations," *Int. J. Heat Fluid Flow*, **21**, pp. 252–263.
- Hanjalic, K., Hadziabdic, M., Temmerman, L., and Leschziner, M., 2004, "Merging LES and RANS Strategies: Zonal or Seamless Coupling?" in *Direct and Large Eddy Simulations V*, R. Friedrich, B. Geurts, and O. Metais, eds., Kluwer Academic Publishers, Dordrecht, pp. 451–464.
- Pope, S. B., 1999, "A Perspective on Turbulence Modeling," in *Modeling Complex Flows*, M. D. Salas, J. N. Hefner, and L. Sakell (eds.), Kluwer Academic Publisher, Dordrecht, pp. 53–67.
- Niceno, B., Dronkers, A. D. T., and Hanjalic, K., 2002, "Turbulent Heat Transfer From a Multi-Layered Wall-Mounted Cube Matrix: an LES," *Int. J. Heat Fluid Flow*, **23**, pp. 173–185.
- Mainders, E., and Hanjalic, K., 1999, "Vortex Structure and Heat Transfer in Turbulent Flow Over a Wall-Mounted Matrix of Cubes," *Int. J. Heat Fluid Flow*, **20**, pp. 255–267.
- Hanjalic, K., and Jakirlic, S., 2002, "Second-Moment Turbulence Closure Modelling," in *Closure Strategies for Turbulent and Transitional Flows*, B. E. Launder and N. Sandham, eds., Cambridge University Press, Cambridge, pp. 47–101.
- Geroyimos, G. A., Neubauer, J., Sharma, V. C., and Vallet, I., 2002, "Improved Prediction of Turbomachinery Flows Using Near-Wall Reynolds-Stress Model," *ASME J. Turbomach.*, **124**, pp. 86–99.
- Craft, T. J., and Launder, B. E., 2002, "Closure Modelling Near the Two-Component Limit," in *Closure strategies for turbulent and transitional flows*, B. E. Launder and N. Sandham, eds., Cambridge University Press, Cambridge, pp. 102–126.
- Leschziner, M. A., and Lien, F.-S., 2002, "Numerical Aspects of Applying Second-Moment Closure to Complex Flows," in *Closure Strategies for Turbulent and Transitional Flows*, B. E. Launder and N. Sandham, eds., Cambridge University Press, Cambridge, pp. 153–187.
- Basara, B., 2004, "Employment of the Second-Moment Turbulence Closure on Arbitrary Unstructured Grid," *Int. J. Numer. Methods Fluids*, **44**(4), pp. 377–408.
- Basara, B., and Jakirlic, S., 2003, "A New Hybrid Modelling Strategy for Industrial CFD," *Int. J. Numer. Methods Fluids*, **42**, pp. 89–116.
- Chassaing, J., Geroyimos, G. A., and Vallet, I., 2003, "Reynolds-Stress Model Dual-Time-Stepping Computation of Unsteady Three-Dimensional Flows," *AIAA J.*, **41**, pp. 1882–1894.
- Yang, S. L., Peschke, D. B., and Hanjalic, K., 2000, "Second-Moment Closure Model for IC Engine Flow Simulation Using KIVA Code," *ASME J. Eng. Gas Turbines Power*, **122**, pp. 355–363.
- Yang, S. L., Siow, Y. K., Teo, C. Y., and Hanjalic, K., 2005, "A KIVA Code With Reynolds-Stress Model for Engine Simulation," *Energy Int. J.*, **30**, pp. 427–445.
- Speziale, C. G., Sarkar, S., and Gatski, T. B., 1991, "Modelling the Pressure Strain Correlation of Turbulence: An Invariant Dynamic System Approach," *J. Fluid Mech.*, **227**, pp. 245–272.
- Wallin, S., and Johansson, A., 2002, "Modelling Streamline Curvature Effects in Explicit Algebraic Reynolds Stress Turbulence Models," *Int. J. Heat Fluid Flow*, **23**, pp. 721–730.
- Durbin, P., 1991, "Near-Wall Turbulence Closure Modeling Without 'Damping Functions,'" *Theor. Comput. Fluid Dyn.*, **3**, pp. 1–13.
- Craft, T. J., Launder, B. E., and Suga, K., 1996, "Development and Application of a Cubic Eddy-Viscosity Model of Turbulence," *Int. J. Heat Fluid Flow*, **17**, pp. 108–115.
- Chen, W. L., Lien, F. S., and Leschziner, M. A., 1998, "Computational Prediction of Flow Around Highly Loaded Compressor-Cascade Blades With Non-Linear Eddy-Viscosity Models," *Int. J. Heat Fluid Flow*, **19**, pp. 307–319.
- Hanjalic, K., Popovac, M., and Hadziabdic, M., 2004, "A Robust Near-Wall Elliptic Relaxation Eddy-Viscosity Turbulence Model for CFD," *Int. J. Heat Fluid Flow*, **25**, pp. 1047–1051.
- Manceau, R., and Hanjalic, K., 2002, "Elliptic Blending Model: A New Near-Wall Reynolds-Stress Turbulence Closure," *Phys. Fluids*, **14**(2), pp. 744–754.
- Durbin, P. A., 1993, "Reynolds Stress Model for Near-Wall Turbulence," *J. Fluid Mech.*, **249**, pp. 465–498.
- Thielen, L., Jonker, H. J., and Hanjalic, K., 2003, "Symmetry Breaking of Flow and Heat Transfer in Multiple Impinging Jets," *Int. J. Heat Fluid Flow*, **24**, pp. 444–453.
- Thielen, L., Hanjalic, K., Jonker, H., and Manceau, R., 2005, "Predictions of Flow and Heat Transfer in Multiple Impinging Jets With an Elliptic-Blending Second-Moment Closure," *Int. J. Heat Mass Transfer*, **48**, pp. 1583–1598.
- Geers, L. F. G., Tummers, M., and Hanjalic, K., 2004, "Experimental Investigation of Impinging Jet Arrays," *Exp. Fluids*, **36**, pp. 946–958.
- Hanjalic, K., Launder, B. E., and Schiestel, R., 1980, "Multiple-Scale Concepts in Turbulent Transport Modelling," in *Turbulent Shear Flow 2*, F. Durst et al., eds., Springer, Berlin, pp. 36–49.
- Schiestel, R., 1987, "Multiple-Time Scale Modeling of Turbulent Flows in One Point Closures," *Phys. Fluids*, **30**(3), pp. 722–731.
- Cadiou, A., Hanjalic, K., and Stawiariski, K., 2004, "A Two-Scale Second-Moment Turbulence Closure Based on Weighted Spectrum Integration," *Theor. Comput. Fluid Dyn.*, **18**, pp. 1–26.
- Temmerman, L., Leschziner, M. A., Hadziabdic, M., and Hanjalic, K., 2005, "A Hybrid Two-Layer URANS-LES Approach for Large-Eddy Simulation at High Reynolds Numbers," *Int. J. Heat Fluid Flow*, **26**, pp. 173–190.
- Schiestel, R., and Dejoan, A., 2005, "Towards a New Partially Integrated Transport Model for Coarse Grid and Unsteady Turbulent Flow Simulations," *Theor. Comput. Fluid Dyn.*, **18**, pp. 443–468.
- Nikitin, N. V., Nocoud, F., Wasistho, B., Squires, K. D., and Spalart, P. R., 2000, "An Approach to Wall Modelling in Large-Eddy Simulations," *Phys. Fluids*, **12**(7), pp. 1629–1632.
- Piomelli, U., Balaras, E., Pasinato, H., Squires, H., and Spalart, P., 2003, "The Inner-Outer Layer Interface in Large-Eddy Simulations With Wall-Layer Models," *Int. J. Heat Fluid Flow*, **24**, pp. 538–550.
- Davidson, L., and Dahlstöm, S., 2004, "Hybrid LES-RANS: An Approach to Make LES Applicable at High Reynolds Number," *Proc. (CD) CHT-04, Int. Symp. on Advances in Computational Heat Transfer*, April 19–25, Norway, ICHMT/Begell House.
- Hadziabdic, M., and Hanjalic, K. (to be published).
- Hanjalic, K., 2002, "One-Point Closure Models for Buoyancy-Driven Turbulent Flows," *Annu. Rev. Fluid Mech.*, **34**, pp. 321–347.
- Kenjereš, S., and Hanjalic, K., 2002, "Numerical Insight Into Flow Structure in Ultraturbulent Thermal Convection," *Phys. Rev. E*, **66**, p. 036307.
- Kenjereš, S., and Hanjalic, K., 2002, "Combined Effects of Terrain Orography and Thermal Stratification on Pollutant Dispersion in a Town Valley: a T-RANS Simulation," *J. Turbul.*, **3**, pp. 1–21.